Designing phase compensation for coherent control of frequency combs via high-order harmonic generation

Chang-Tong Liang,[1,2,3] Yu-Hang He,[1,2] Ming-Gen Li,[1,2] and Peng-Cheng Li[1,2,*]

[1]*Department of Physics, College of Science, Shantou University, Shantou, Guangdong 515063, China*

[2]*Key Laboratory of Intelligent Manufacturing Technology of MOE, Shantou University, Shantou, Guangdong 515063, China*

[3]*Institute of Applied Physics and Computational Mathematics, Beijing 100088, China*

(Received 1 February 2024; accepted 26 June 2024; published 10 July 2024)

We present a phase-compensation rule for achieving coherent control of frequency combs via high-order harmonic generation (HHG). The phase-compensation rule is illustrated by performing the generation of frequency combs via HHG from a hydrogen atom subjected to an intense laser pulse train. The numerical technique involves accurate and efficient solution of the time-dependent Schrödinger equation by means of the time-dependent generalized pseudospectral method. The results indicate that the frequency combs are fully optimized by employing the proposed phase-compensation rule, allowing direct control and generation of frequency combs with either the regular structure or the denser repetition combs. The performance of phase compensation is evaluated by analyzing the dynamical evolution of the harmonic spectra driven by several phase-compensation schemes. We believe that our findings serve as a guide for the experimental realization of phase coherent control of frequency combs via HHG at extremely high repetition frequencies.

DOI: 10.1103/PhysRevA.110.013506

I. INTRODUCTION

Frequency combs (FCs) are generated by a precisely regular sequence of laser pulses, resulting in an optical spectrum composed of evenly spaced spectral lines that repeat [1,2]. FCs provide a highly accurate and versatile frequency reference with applications in time-frequency metrology [3], direct frequency-comb spectroscopy [4], and sensing, coherent control of atomic, molecular, and optical systems [5,6]. Expanding the range of FCs into the extreme ultraviolet (XUV) spectral region is of great interest, as it would enable wide-bandwidth frequency metrology and facilitate innovative tests in quantum electrodynamics [7,8]. Accessing this high-bandwidth comb directly is hindered by the limited power of single-frequency lasers and the lack of media for frequency up-conversion. However, coherent high-order harmonic generation (HHG) from atomic and molecular systems driven by intense laser pulse trains offers a viable method for realizing XUV FCs in both theoretical and experimental studies [9,10].

In recent studies, Kandula *et al.* [11] demonstrated the generation of FCs in the XUV region. Carrera *et al.* [12] investigated the influence of pulse number and laser intensity on the structure of FCs generated through HHG. Our team also reported the coherent enhancement of FCs by combining infrared laser pulses with terahertz (THz) laser fields [13]. However, achieving higher average power and pulse repetition rates in HHG remains a challenge. The intensity required for HHG with repetition rates exceeding 100 MHz demands lasers with average powers of several kilowatts [14]. Such a power level can be attained through laser amplification technologies like chirped-pulse amplification [15], optical parametric chirped-pulse amplification [16,17], and femtosecond enhancement cavities [18,19]. To increase the repetition rates and drive HHG efficiently, it is desirable to employ shorter laser pulses [20,21]. However, for few-cycle pulses, the accurate stabilization of the carrier-envelope phase (CEP) becomes crucial [22], as the CEP effects significantly impact the generation of precision FCs [23,24].

In addition, the pulse repetition rates have an inverse relationship with the time interval between consecutive pulses, which corresponds to the repetition frequency of the FCs. This parameter is crucial in determining the precision of FCs [25]. Femtosecond enhancement cavities are commonly employed by various laboratories for XUV frequency comb generation [19]. These cavities ensure that the coherence property of the fundamental drive laser is effectively transferred to the XUV with the original repetition frequency of the FCs [14]. Therefore, controlling the coherence of the laser pulses on short timescales is a direct approach to achieving higher precision FCs [20]. However, by increasing the pulse repetition rates to attain higher-precision FCs, it presents challenges due to limitations in average laser power and single-pulse intensity [26]. Previous works [27] have investigated the potential limitations of decreasing pulse duration to increase the repetition rate in HHG. The structure of the harmonic FCs arises from quantum interferences among induced dipole pulses [28,29].

This paper presents a phase-compensation rule designed to control the coherence of FCs generated through HHG. The aim is either to improve the repetition combs or optimize the structure of the FCs. The phase-compensation rule is evaluated by analyzing the dynamical evolution of the harmonic spectra driven by various phase-compensation

*Contact author: pchli@stu.edu.cn

schemes. Based on the dynamical evolution of FCs via HHG under the given phase-compensation schemes, we find the general phase-compensation rule for the generation of FCs via HHG with either regular structures or the denser combs.

This paper is organized as follows. In Sec. II, we briefly introduce the theoretical methods. In Sec. III, the phase-compensation rule designed to control the coherence of FCs generated through HHG is discussed. Section IV contains concluding remarks.

II. THEORETICAL METHOD

To demonstrate the phase-compensation rule, we employ the laser pulse train as the driving laser field for the laser-atom interaction. This process can be treated by solving the time-dependent Schrödinger equation (TDSE) in atomic units:

$$i\frac{\partial\psi(\mathbf{r},t)}{\partial t} = H\psi(\mathbf{r},t) = [H_0 + V(\mathbf{r},t)]\psi(\mathbf{r},t), \quad (1)$$

where H_0 represents the unperturbed Hamiltonian of the hydrogen atom, and $V(\mathbf{r},t)$ is the time-dependent interaction of the electron with the laser field in the dipole approximation:

$$V(\mathbf{r},t) = -\mathbf{E}(\mathbf{t})\cdot\mathbf{r} = -zE(t). \quad (2)$$

Here, $E(t)$ is the laser pulse train defined as [30]

$$E(t) = \sum_{n=1}^{N} E_0 F(t-n\tau)\exp[i(\omega_c t - n\omega_c\tau + n\Delta\phi)], \quad (3)$$

E_0 is the peak amplitude of the laser field, $F(t-n\tau)$ is the Gaussian envelope function which can be expressed as $F(x) = \exp[-2(ln2)x^2/{\tau_0}^2]$, τ_0 is the full width at half maximum, N is the number of laser pulses, and the pulse-to-pulse phase shift is given by $\Delta\phi$. To accurately and efficiently solve the TDSE in spherical coordinates, we employ the time-dependent generalized pseudospectral (TDGPS) method [31]. The TDGPS method utilizes the generalized pseudospectral technique for nonuniform optimal spatial discretization of the coordinates and the Hamiltonian using only a modest number of grid points. The time propagation of the wave function under this method is carried out using the split operator method [32] in the energy representation:

$$\psi(\mathbf{r},t+\Delta t) \simeq \exp\left(-iH_0\frac{\Delta t}{2}\right)\exp\left[-iV\left(t+\frac{\Delta t}{2}\right)\Delta t\right] \times \exp\left(-iH_0\frac{\Delta t}{2}\right)\psi(\mathbf{r},t) + O(\Delta t^3). \quad (4)$$

Once the time-dependent wave function is obtained, the time-dependent induced dipole moment in the length and acceleration forms can be calculated as

$$d_L(t) = \langle\psi(\mathbf{r},t)|z|\psi(\mathbf{r},t)\rangle, \quad (5)$$

$$d_A(t) = \langle\psi(\mathbf{r},t)|-\frac{z}{r^3}+E(t)|\psi(\mathbf{r},t)\rangle. \quad (6)$$

The FC spectra via HHG can be obtained as follows:

$$P(\omega) = \frac{2\omega^4}{3\pi c^3}|\tilde{d}(\omega)|^2, \quad (7)$$

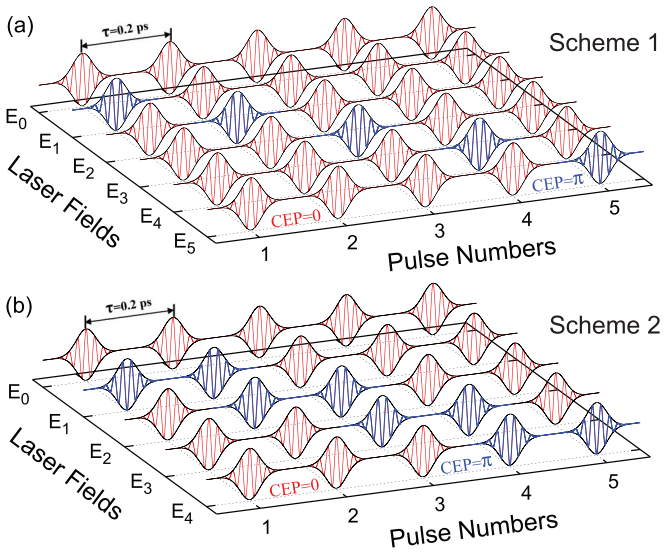

FIG. 1. Schematics of phase compensation for laser pulse trains. (a) Phase-compensation scheme 1 involves the phase design between each laser pulse by changing the phase of one laser pulse with the given CEP (blue solid lines) in the laser pulse train. Here, E_0 denotes the phase without compensation for each pulse, while E_1, E_2, E_3, E_4, and E_5 represent different cases of phase compensation. (b) Phase-compensation scheme 2 involves the phase design between each laser pulse by changing the phase of two laser pulses with the given CEP in the laser pulse train.

where $\tilde{d}(\omega)$ is the Fourier transformation of the induced dipole moment in the acceleration form $d_A(t)$ divided by the number of pulses N to scale to the one-pulse case [29,31]:

$$\tilde{d}(\omega) = \frac{1}{N\omega^2}\int_{-\infty}^{\infty} d_A(t)e^{-i\omega t}dt = \frac{1}{N}\sum_{n=1}^{N}\tilde{d}_n(\omega), \quad (8)$$

and $\tilde{d}_n(\omega)$ is the spectral dipole moment calculated by the nth dipole pulse.

III. RESULTS AND DISCUSSIONS

FCs' structure of the harmonics arises from quantum interferences among induced spectral dipole moments, and this fundamental pattern remains unchanged regardless of the values of the pulse number N [12,28]. In this work, we focus on the designing of phase-compensation schemes using five laser pulse trains. Figures 1(a) and 1(b) show two different types of schematics for phase compensation of laser pulse trains. In Fig. 1(a), the phase compensation is achieved by changing the phase of one laser pulse (blue solid lines) with a specified carrier-envelope phase (CEP) π between four successive laser pulses (red solid lines) as indicated by scheme 1. The phase without compensation for each pulse is denoted as E_0, and the different cases of phase compensation are represented by E_1, E_2, E_3, E_4, and E_5. In Fig. 1(b), the phase compensation is achieved by changing the phase of two laser pulses with the given CEP between three successive laser pulses (red solid lines), as indicated by scheme 2.

Figure 2(a) shows the FCs (pattern filled in red) near the 19th harmonic and the corresponding spectral phase without

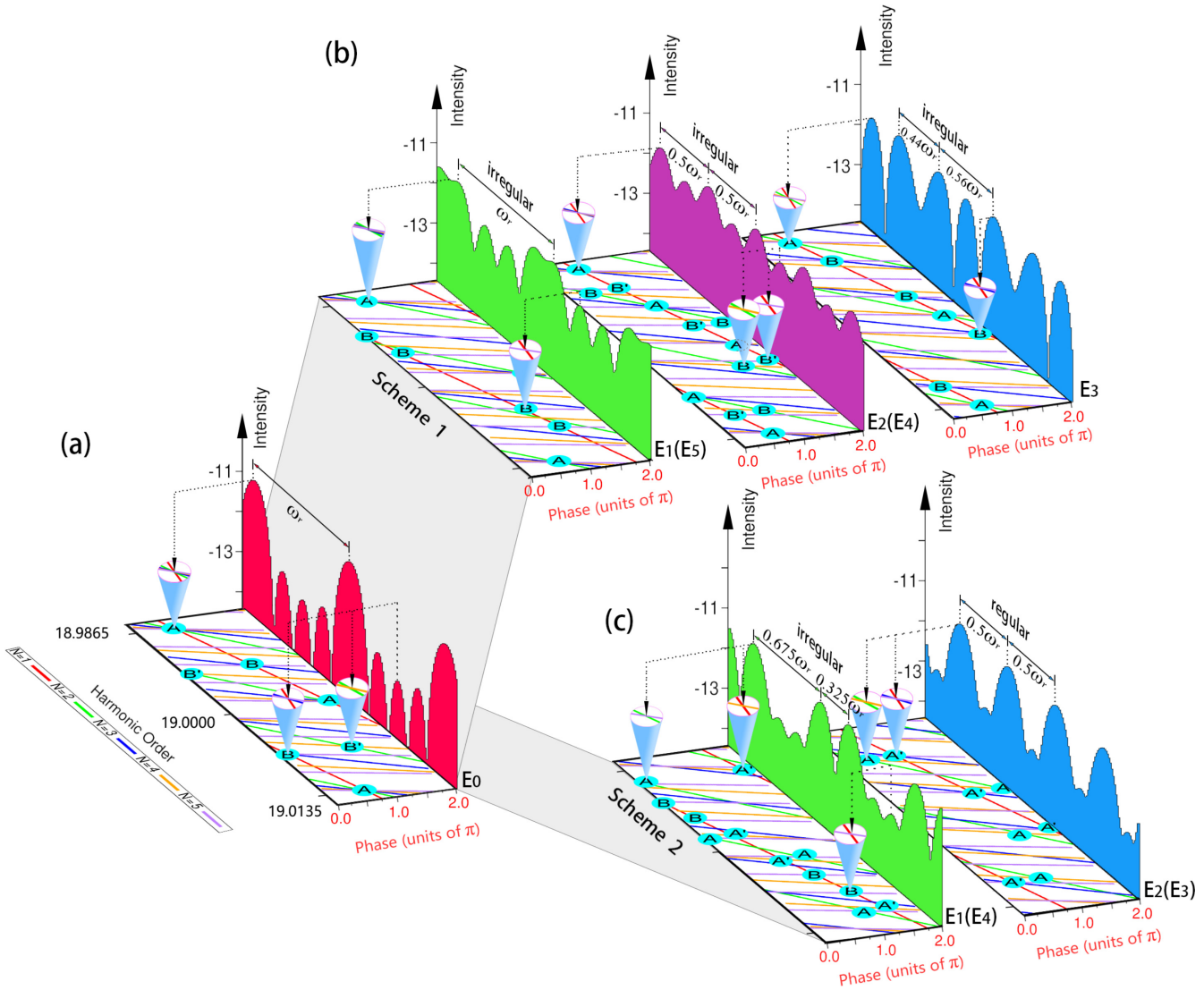

FIG. 2. FCs (pattern filled in red) near the 19th harmonic and the corresponding spectral phase (pattern with lines) for the phase-compensation schemes 1 and 2 as shown in Figs. 1(a) and 1(b), respectively. For comparison, the FCs via HHG without the phase-compensation case are depicted in panel (a). Panels (b) and (c) represent schemes 1 and 2, respectively. The driving laser field comprises five consecutive pulses ($N = 5$) with an intensity of 0.8×10^{14} W/cm^2. The laser wavelength used is 800 nm with a FWHM at 15 fs, and N is the number of pulses. The quantum coherence of FCs are presented by the phases intersecting, marked by labels A (A′) and B (B′); the conical cross section indicates the zoomed-in view of the intersection of several coherent phases of FCs. ω_r is the repetition frequency of FCs. The notations E_0, E_1, E_2, E_3, E_4, and E_5 have the same meanings as those shown in Fig. 1.

the phase-compensation case E_0. In the simulation, the driving laser field comprises five consecutive pulses ($N = 5$) with an intensity of 0.8×10^{14} W/cm^2. The laser wavelength used is 800 nm with a full width at half maximum (FWHM) at 15 fs, and the repetition rate f_{rep} used is 5 THz ($\tau = 0.2$ ps). The repetition rate f_{rep} means pulse repetition frequency of the pulse laser train; it is defined as the number of pulses emitted every second, or the inverse temporal pulse spacing τ, and it is inversely proportional to the pulse energy and directly proportional to the average power. Higher repetition rates result in less thermal relaxation time at the focused spot, which leads to more rapid material heating. The laser parameters used are now available and provide a valuable research tool for efficiently driving multiphoton processes.

The spectral phase $\theta_n(\omega)$ is defined as the argument of the Fourier transformation of the induced dipole moment shown in Eq. (8):

$$\theta_n(\omega) = \arg[\tilde{d}_n(\omega)]. \tag{9}$$

For the FCs via HHG without phase compensation, the structure of FCs includes a group of combs containing two higher peaks and three interference substructures. The spectral phases are represented as follows: red lines for the laser pulse $N = 1$, green lines for $N = 2$, blue lines for $N = 3$, yellow lines for $N = 4$, and violet lines for $N = 5$. The phase intersecting, marked by A, B, and B′, denote the quantum coherence of the FCs. Note that the conical cross-section indicates the zoomed-in view of

several coherent phases intersecting. The phase intersecting means the same phases of harmonics generated by the different pulses of laser trains. It implies that the phase-matched harmonics are generated by the nth laser pulses. The phase matching is very important to the enhancement of frequency combs, and it is responsible for the frequency-comb structures. The label A represents all five phases intersecting completely and indicates that the harmonic phases are fully coherent, which leads to one high-pulse harmonic. The label B represents three phases intersecting, and B′ represents two phases intersecting. The phase coherence marked by B and B′ contributes to the same peaks of FCs. This implies that the generation of FCs may come from two coherent channels for E_0 without phase compensation. The comb frequencies are determined by $\omega_k = k\omega_r + \omega_0$, where k is an integer index, ω_r is the repetition frequency, and ω_0 is the offset frequency [12,28]. ω_r represents the spacing between adjacent high FC peaks in HHG on the frequency scale. In Fig. 2(a), ω_r is equal to 5.0 THz, corresponding to the frequency range from the harmonic order 18.9865 to 19.00 (0.0135 harmonic orders) for a carrier wavelength of 800 nm.

Figure 2(b) depicts the FCs obtained via HHG with phase-compensation cases E_1 (E_5) in scheme 1. In this cases, the structure of FCs consists of a group of combs containing two higher peaks and two interference substructures. The spacing between adjacent high peaks is equal to 0.0135 harmonic orders, corresponding to a repetition frequency ω_r of 5 THz. However, the FCs' structure is irregular. The label A represents four phases intersecting and the label B represents two phases intersecting. This indicates that the phase-compensation cases E_1 (E_5) have two kinds of phase coherence. For the FCs via HHG with the phase-compensation case E_2 (E_4) in scheme 1, the structure of FCs includes a group of combs containing two higher peaks and one interference substructure. The label A represents four phases intersecting and the labels B and B′ represent two phases intersecting, respectively. The repetition frequency is $0.5\omega_r$ (0.006 75 harmonic orders) with irregular FC structure. For the phase-compensation case E_3, the structure of FCs includes a group of combs containing three higher combs without interference substructures. The frequency space of the FC is $0.44\omega_r$ and $0.56\omega_r$, respectively. The label A represents four phases intersecting and the label B represents three phases intersecting. Although the cases E_1 (E_5) and E_3 have similar coherent channels A with four phases intersecting, the intersecting of these phases comes from the different driven-laser cases, so the structures of the FCs are different.

Figure 2(c) displays the FCs near the 19th harmonic and their corresponding spectral phases for the phase compensation in scheme 2, as shown in Fig. 1(b). For the FCs obtained via HHG with the phase-compensation case E_1 (E_4), the structure of FCs includes a group of spectra containing three intense combs with $0.675\omega_r$ and $0.325\omega_r$, and the structure of the FCs is irregular. The higher peaks of the FCs have spectral phases originating from two coherent channels, labeled as A and A′. The low substructures only have one coherent phase channel, labeled as B. In the case of FCs obtained via HHG with the phase-compensation case E_2 (E_3), the structure of the FCs includes a group of spectra containing two high peaks and one very low subpeak. The repetition frequency is $0.5\omega_r$ by comparing with the case E_0, and the structure of the FCs is very regular. All spectral phases originate from two coherent channels, A and A′, where channel A represents two phases intersecting and channel A′ represents three phases intersecting. This implies that two different types of phase coherence contribute to the main spectral peaks in the phase-compensation case E_2 (E_3), which leads to regular FC structures. Within a certain frequency range, the smaller the interval between two comb teeth, the more comb teeth there are, indicating the denser repetition combs of the FCs.

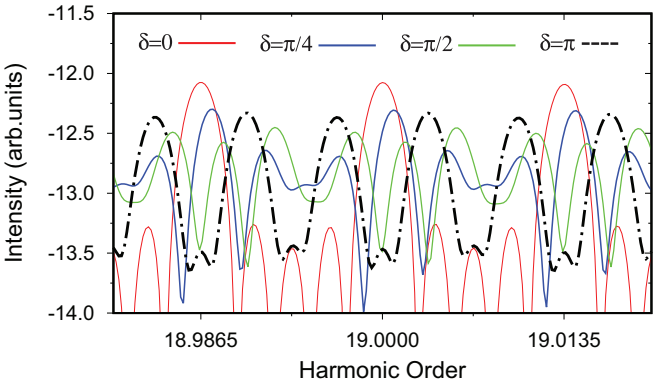

FIG. 3. FCs near the 19th harmonic with the variations δ ($|\Omega_1 - \Omega_2|$) of the neighbor phase difference of two laser pulses.

From the discussions about Figs. 2(b) and 2(c), it is apparent that the structure and the repetition frequency of the FCs can be manipulated through phase compensation of the laser pulse train. Based on the analysis of the phase-compensation schemes 1 and 2, we have derived a general rule for phase compensation in arbitrary laser pulse trains, which can be expressed as follows:

$$\phi_n - \phi_{n-1} = \Omega_1 \;\; \phi_{n+1} - \phi_n = \Omega_2, (n = 2, 3, 4, \ldots, N),$$
$$\delta = |\Omega_1 - \Omega_2| = \pi, \tag{10}$$

where ϕ_n is the phase of the arbitrary laser pulse, n is the index of laser pulses ($n \geqslant 2$), and Ω_1 and Ω_2 denote the phase difference of the arbitrary two adjacent laser pulses. δ is the subtraction of the neighbor phase difference of two laser pulses. The phase compensation is good only when δ is specifically equal to a constant π.

To confirm the rule of the phase compensation as shown in Eq. (10), we present the FCs near the 19th harmonic with the variations δ ($|\Omega_1 - \Omega_2|$) of the neighbor phase difference of two laser pulses. Here, the choice of the phase of the first pulse ϕ_1 and the second pulse ϕ_2 may be arbitrary, leading to the arbitrariness of Ω_1 and Ω_2. δ is equal to 0, $\pi/4$, and $\pi/2$ as shown in Fig. 3 . For the reference, we present that the δ is equal to π. We find that, only for $\delta = \pi$, the FCs either have the regular structure or the denser repetition combs. Therefore, the phase-compensation rule is a general principle. In addition, we find that the intensity of harmonic spectra will be lower while the δ is not equal to zero. This implies that the quantum interferences not only affect the FC structure but also affect the intensity of the frequency comb spectra, and similar results can be found in Ref. [29].

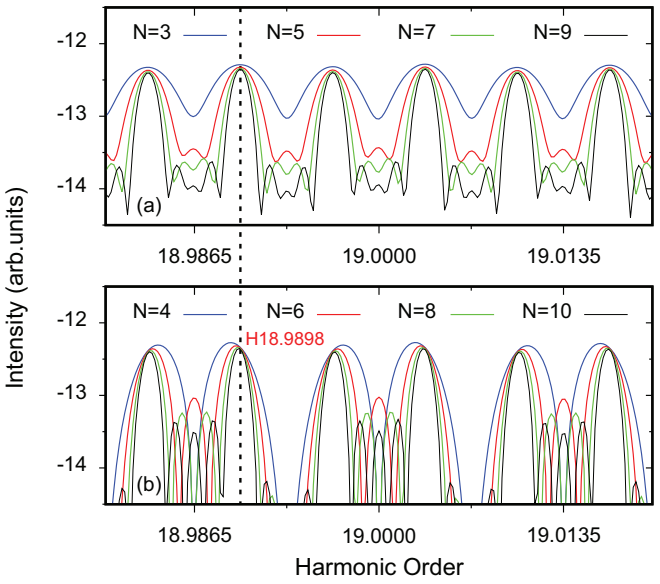

FIG. 4. FCs near the 19th harmonic are shown for the phase-compensation case E_2 (E_3) with the changing number of laser pulse trains in scheme 2. (a) For the odd laser pulse trains. (b) For the even laser pulse trains.

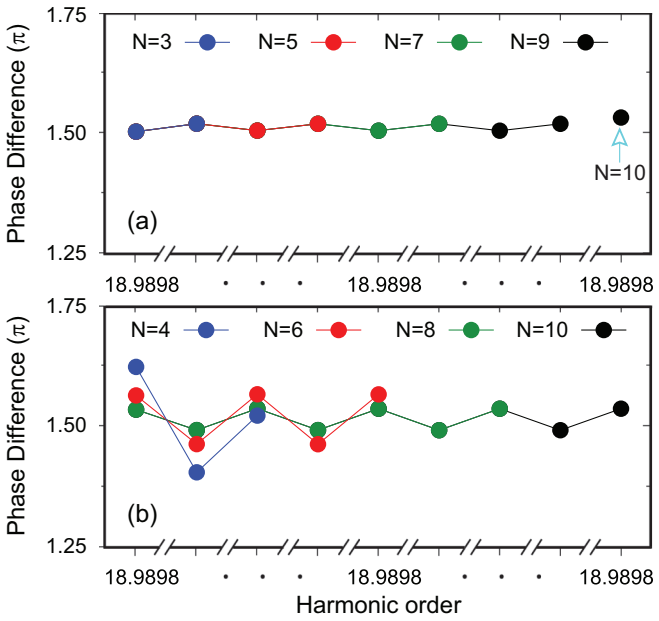

FIG. 5. Phase differences of FCs in the vicinity of the 19th harmonic (H18.9898) marked by the black dashed line in Fig. 4. (a) For the odd laser pulse trains. (b) For the even laser pulse trains.

In Figs. 4(a) and 4(b), we check the sensitivity of the phase compensation to the number N of the laser pulse, we show the FCs near the 19th harmonic for the phase compensation E_2 (E_3) in scheme 2 when the number of laser pulse trains is changed. For the case of the odd pulse trains, results similar to those of the discussion above have been obtained. For the case of the even pulse trains, the peaks of FCs appear to shift, and the shift is very obvious in the case of the small pulse number N, but the structures of FCs with phase compensation cannot be changed when the number N is larger than 10. It is demonstrated that the schemes of phase compensation produce a more stable FC structure in a larger number of laser pulse trains.

To explain the spectra shift of FCs in the case of a small even number of laser pulse trains, we calculate the phase differences of FCs in the vicinity of the 19th harmonic (H18.9898) marked by the black dashed line in Fig. 4 in the cases of either the odd pulse trains or the even pulse trains, respectively. In calculation, the harmonic spectral phase differences can be obtained by Eq. (9). For the phase differences of FCs generated by the odd pulse trains as shown in Fig. 5(a), the values are always located at around 1.5π. However, for the phase differences of FCs generated by the even pulse trains as shown in Fig. 5(b), the values have a sharp oscillation in the case of a smaller number of laser pulse trains. The phase differences of FCs are closing 1.5π with increasing the number of laser pulse trains, and it becomes more stable when the number of laser pulse trains is larger than 10. For the comparison, the phase difference of FCs generated by ten laser pulse trains ($N = 10$) is marked by an arrow in Fig. 5(a). Our results indicate that the coherent interference from the unstable phase differences of each adjacent laser pulse leads to the shift of comb teeth.

IV. CONCLUSION

In summary, we have established a phase-compensation rule by analyzing the dynamical evolution of the harmonic spectra driven by various phase-compensation schemes. This rule represents a general approach for phase coherent control of FCs via HHG driven by a larger number of pulse trains. Our results demonstrate that the FCs can be fully optimized by applying the designed phase-compensation rule, facilitating direct control and generation of FCs with either regular structure or denser repetition combs, and this FC structure appears within each of the harmonics, ranging from the first harmonic to the cutoff harmonic. Obviously, the proposed phase difference in adjacent pulses, for $\delta = \pi$, can easily be implemented in experiments. Our findings contribute to a comprehensive understanding of the fundamental physics underlying the manipulation of the frequency-comb structure through phase compensation, offering valuable insights for experiments aiming to achieve high-precision FCs in the vacuum ultraviolet regions. We believe that this method proposed can be extended to other systems and can provide an efficient method for the production of the optimizing FCs.

ACKNOWLEDGMENT

This work supported by the National Natural Science Foundation of China (Grant No. 12074239), Li Ka Shing Foundation STU-GTIIT Joint Research Grants (Grant No. 2024LKSFG02), and the STU Scientific Research Foundation for Talents (Grants No. NTF22026, No. NTF23011, No. NTF23014, and No. NTF23036T).

[1] Th. Udem, R. Holzwarth, and T. W. Hänsch, Nature (London) **416**, 233 (2002).
[2] S. T. Cundiff and J. Ye, Rev. Mod. Phys. **75**, 325 (2003).
[3] N. Picqué and T. W. Hänsch, Nat. Photon. **13**, 146 (2019).
[4] M. C. Stowe, M. J. Thorpe, A. Pe'er, J. Ye, J. E. Stalnaker, V. Gerginov, and S. A. Diddams, Adv. At., Mol. Opt. Phys. **55**, 1 (2008).
[5] M. C. Stowe, F. C. Cruz, A. Marian, and J. Ye, Phys. Rev. Lett. **96**, 153001 (2006).
[6] A. Pe'er, E. A. Shapiro, M. C. Stowe, M. Shapiro, and J. Ye, Phys. Rev. Lett. **98**, 113004 (2007).
[7] A. Cingöz, D. C. Yost, T. K. Allison, A. Ruehl, M. E. Fermann, I. Hartl, and J. Ye, Nature (London) **482**, 68 (2012).
[8] I. Pupeza, C. Zhang, M. Högner, and J. Ye, Nat. Photon. **15**, 175 (2021).
[9] F. Lindner, W. Stremme, M. G. Schätzel, F. Grasbon, G. G. Paulus, H. Walther, R. Hartmann, and L. Strüder, Phys. Rev. A **68**, 013814 (2003).
[10] C. Gohle, Th. Udem, M. Herrmann, J. Rauschenberger, R. Holzwarth, H. A. Schuessler, F. Krausz, and T. W. Hänsch, Nature (London) **436**, 234 (2005).
[11] D. Z. Kandula, C. Gohle, T. J. Pinkert, W. Ubachs, and K. S. E. Eikema, Phys. Rev. Lett. **105**, 063001 (2010).
[12] J. J. Carrera, S.-K. Son, and S.-I Chu, Phys. Rev. A **77**, 031401(R) (2008).
[13] Y. Y. Wu, C. T. Liang, B. G. Zhao, and P. C. Li, Phys. Rev. A **108**, 043101 (2023).
[14] R. J. Jones, K. D. Moll, M. J. Thorpe, and J. Ye, Phys. Rev. Lett. **94**, 193201 (2005).
[15] S. Backus, C. G. Durfee, M. M. Murnane, and H. C. Kapteyn, Rev. Sci. Instrum. **69**, 1207 (1998).
[16] R. Won, Nat. Photon. **4**, 207 (2010).
[17] O. Chalus, P. K. Bates, M. Smolarski, and J. Biegert, Opt. Express **17**, 3587 (2009).
[18] D. C. Yost, T. R. Schibli, and Jun Ye, Opt. Lett. **33**, 1099 (2008).
[19] T. K. Allison, A. Cingöz, D. C. Yost, and J. Ye, Phys. Rev. Lett. **107**, 183903 (2011).
[20] H. Carstens, N. Lilienfein, S. Holzberger, C. Jocher, T. Eidam, J. Limpert, A. Tünnermann, J. Weitenberg, D. C. Yost, A. Alghamdi, Z. Alahmed, A. Azzeer, A. Apolonski, E. Fill, F. Krausz, and I. Pupeza, Opt. Lett. **39**, 2595 (2014).
[21] I. Pupeza, S. Holzberger, T. Eidam, H. Carstens, D. Esser, J. Weitenberg, P. Rußbüldt, J. Rauschenberger, J. Limpert, Th. Udem, A. Tünnermann, T. W. Hänsch, A. Apolonski, F. Krausz, and E. Fill, Nat. Photon. **7**, 608 (2013).
[22] G. G. Paulus, F. Grasbon, H. Walther, P. Villoresi, M. Nisoli, S. Stagira, E. Priori, and S. De Silvestri, Nature (London) **414**, 182 (2001).
[23] D. J. Jones, S. A. Diddams, J. K. Ranka, A. Stentz, R. S. Windeler, J. L. Hall, and S. T. Cundiff, Science **288**, 635 (2000).
[24] S. Holzberger, N. Lilienfein, M. Trubetskov, H. Carstens, F. Lücking, V. Pervak, F. Krausz, and I. Pupeza, Opt. Lett. **40**, 2165 (2015).
[25] N. R. Newbury, Nat. Photon. **5**, 186 (2011).
[26] G. Porat, C. M. Heyl, S. B. Schoun, C. Benko, N. Dörre, K. L. Corwin, and J. Ye, Nat. Photon. **12**, 387 (2018).
[27] H. Carstens, M. Högner, T. Saule, S. Holzberger, N. Lilienfein, A. Guggenmos, C. Jocher, T. Eidam, D. Esser, V. Tosa, V. Pervak, J. Limpert, A. Tünnermann, U. Kleineberg, F. Krausz, and I. Pupeza, Optica **3**, 366 (2016).
[28] M. Tudorovskaya and M. Lein, Phys. Rev. A **95**, 043418 (2017).
[29] C. T. Liang, Y. Y. Wu, Z. B. Wang, and P. C. Li, Opt. Express **30**, 2413 (2022).
[30] J. J. Carrera and S.-I Chu, Phys. Rev. A **79**, 063410 (2009).
[31] X.-M. Tong and S.-I Chu, Chem. Phys. **217**, 119 (1997).
[32] M. R. Hermann and J. A. Fleck, Phys. Rev. A **38**, 6000 (1988).